Article

Membrane theory prediction is fully against experimental facts

Hirohisa Tamagawa [1,*] **and Bernard Delalande** [2]

[1] Department of Mechanical Engineering, Faculty of Engineering, Gifu University, 1-1 Yanagido, Gifu, Gifu, 501-1193 Japan; tmgwhrhs@gifu-u.ac.jp
[2] 280 avenue de la Pierre Dourdant, 38290 La Verpilliere, France; bernard@somasimple.com
* Correspondence: tmgwhrhs@gifu-u.ac.jp; Tel.: +81-58-293-2529 (H.T.)

Abstract: Accurate prediction of the membrane potential by membrane theory is possible on the basis that the plasma membrane is selectively permeable to ions and that permeability determines the characteristics of the membrane potential. However, an experimental and artificial cell system with an impermeable membrane serving as a model plasma membrane has a non-zero membrane potential, and this potential generated across the membrane is somehow consistent with the potential characteristics predicted by the membrane theory, despite the impermeability of the membrane to ions. A long-forgotten theory, called the association-induction hypothesis (AIH), has emerged as a more plausible mechanism for generating the membrane potential than the membrane theory to explain this unexpected behavior. The AIH asserts that ion-selective membrane permeability is not necessary for the generation of the membrane potential, which is contrary to the membrane theory. Although such an idea is not easy to accept, the experimental results clearly suggest the correctness of the AIH.

Keywords: membrane theory; Association-Induction Hypothesis; ion transport, ion adsorption; membrane potential

1. Introduction

There is a fairly common notion that the membrane potential is generated by trans-membrane ion transport [1]. This physiological notion is even formulated mathematically with the Goldman-Hodgkin-Katz equation (GHK eq.) [1–3]. The GHK equation contains a property called the permeability coefficient. It represents the degree of permeability of the membrane to mobile ions. For more than half a century, countless reports have been published on the experimentally observed membrane potential, which could be quantitatively theorised by the GHK equation. But what about the behaviour of the membrane potential when the permeability of the membrane is zero, i.e. when the membrane is impermeable. Eq. 1 is a typical GHK eq. that every textbook presents. If the membrane is impermeable, all P_i are zero. This means that Eq. 1 is no longer valid.

$$\phi = -\frac{kT}{e} ln \frac{P_{Na}[Na^+]_i + P_K[K^+]_i + P_{Cl}[Cl^-]_o}{P_{Na}[Na^+]_o + P_K[K^+]_o + P_{Cl}[Cl^-]_i} \quad (1)$$

The author has previously found that the potential across the impermeable wire separating two aqueous KCl solutions obeys the prediction of GHK eq. by giving hypothetical non-zero values in the P_i of GHK eq. [4] although P_i should be zero when the impermeable separator is used. It could be argued that introducing a hypothetical value in P_i is an inappropriate use of the GHK eq. and that only the experimentally determined value can be used as P_i. Hence, one may say that GHK eq. should not be used when the impermeable separator is used. However, P_i is often the case determined so that the GHK eq. such as Eq. 1 can reproduce the experimentally measured potential. Thus, usually, P_i is estimated rather than experimentally determined. This point is discussed in our previous paper ref. [4], too. Apart from the GHK equation and electrophysiology, electrostatics suggests that there should be a non-zero potential as long as there is a non-zero charge, and non-zero charges exist in a living cell in the form of ions. This means that a non-zero potential is

Citation: Tamagawa, H.; Delalande B. Membrane theory prediction. *Preprints* **2021**, *1*, 0. https://doi.org/

Received:
Accepted:
Published:

inevitably generated even if the ions never cross the plasma membrane, and this non-zero potential should also be called the "membrane potential". If it is not the membrane potential, how can we interpret this non-zero potential generated by ions that do not cross the plasma membrane? Experimental evidence and theoretical considerations suggest that the generation of the membrane potential does not require non-zero membrane permeability. However, when it comes to the membrane potential in current electrophysiology, non-zero membrane permeability is a fundamental precondition. There is something that does not work or is absent in current electrophysiology, and yet we have continuously questioned the validity of the membrane theory until today [4–7]. This doubt, not only about the mechanism of generation of the membrane potential, but also about the actual electrophysiology itself, has been continuously raised by some research groups even today [8–14].

Although all physiology textbooks state that transmembrane ion transport is the origin of the membrane potential, we believe that there is a fundamental need to re-examine this. It is by no means a finished research topic, even today. Because of this background, we have studied the mechanism of generation of the membrane potential by using a rather simple experimental work.

2. Materials

2.1. Preparation of electrolytic solutions

A $1M$ KCl solution was prepared by dissolving KCl in deionized water. Then a $10^{-1}M$ KCl solution was prepared by diluting the $1M$ KCl solution by a factor of 10. In the same way, 10^{-2} M, 10^{-3} M and $10^{-4}M$ KCl solutions were prepared. Similarly, $1M$ and $10^{-4}M$ solutions of $NaCl$ and $CaCl_2$ were prepared.

2.2. Preparation of $AgCl-$wire

A polished Ag wire was submerged in bleach and left untouched for 1 hour, resulting in a $AgCl$-coated Ag wire. Then it was washed with deionized water. This $AgCl$-coated Ag wire is to be called $AgCl-$wire.

2.3. Preparation of membranes

Three types of separators made of Ag plate coated with silver oxide were prepared. The following procedure prepares the one: a silver plate $1cm\times1cm$ was submerged into bleach and left untouched for 1 hour to form the silver oxide coat on the Ag plate. Then, we washed it with deionized water. We prepared the next one by the same procedure using a $1cm\times1cm$ silver plate, but it has a 0.3mm-diameter hole at its center. Finally, we prepared the last one by the same procedure using a $1cm\times1cm$ silver plate, but it has a 2mm-diameter hole at its center. These three silver plates are denoted by Nohole-memb, 0.3hole-memb and 2hole-memb, respectively. These separators cannot, of course, be considered as real membranes. But to facilitate the discussion from now on, it is better to call them "membranes".

3. Measurements

3.1. Calibration curve preparation

Once the $AgCl-$wire is immersed in a KCl solution, the Cl^- will be adsorbed at its surface [15], the $AgCl-$wire will generate a non-zero potential which depends on the KCl concentration, and this potential, as a function of the KCl concentration, presents a proportional relationship [16]. Therefore, it is possible to know the concentration of KCl by measuring the potential of the $AgCl-$wire immersed in the solution. The aim is to obtain a calibration curve “Potential of $AgCl-$wire as a function of $[KCl]$”. We carried out the measurement of the potential of the $AgCl-$wire immersed in the KCl solutions, which are prepared in the section 2.1, using the set-up illustrated in Fig. 1.

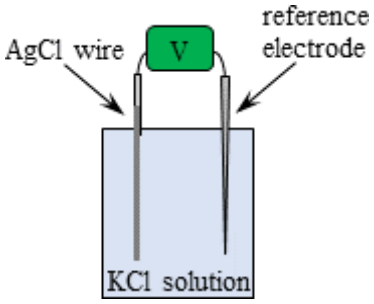

Figure 1. Experimental setup for measuring the *KCl* solution potential

3.2. Potential and ion concentration measurement

Two *KCl* solutions ($1M$ *KCl* and $10^{-4}M$ *KCl*) were separated by a Nohole-memb as shown in Fig. 2, and the potential difference, V_{KCl}, between the two *KCl* solutions was measured as a function of time. The same potential measurement was performed using a 0.3-hole memb and a 2-hole memb. V_L and V_R in Fig. are the potentials of the $AgCl-$ wires immersed in the left *KCl* solution and the right *KCl* solution, respectively. The experimental system shown in Fig.2, when *KCl* solutions are used, is designated by $KCl-$sys. The potentials measured in the $KCl-$sys reflect the Cl^- concentration as described in section 3.1. We performed the same measurements using *NaCl* solutions and $CaCl_2$ solutions. When *NaCl* or $CaCl_2$ solutions are used, the system is designated by $NaCl-$sys or $CaCl_2-$sys, respectively.

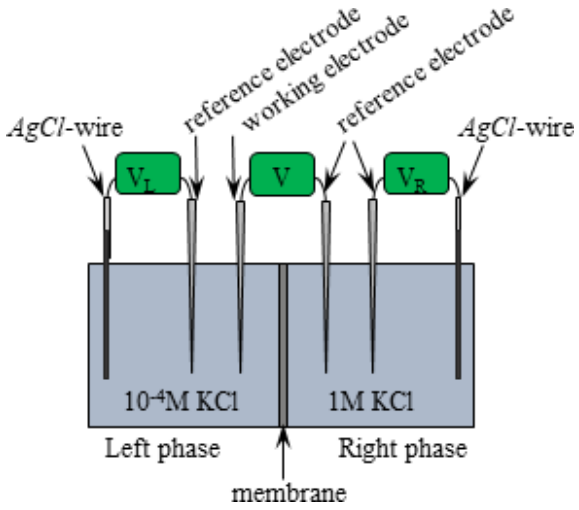

Figure 2. Experimental setup for measuring the potential difference across a membrane (Nohole-memb, 0.3hole-memb, 2hole-memb)

4. Results and Discussion

4.1. Calibration curve for [KCl] and AIH

The relationship $AgCl-$wire potential vs. $-\log_{10}[KCl]$ was obtained experimentally by the method described in section 3.1, and the result is shown in Fig. 3. Figure 3 suggests that there is a virtually proportional relationship between the potential of the $AgCl-$wire and $-\log_{10}[KCl]$. Therefore, the *KCl* concentration of any *KCl* solution is predictable by measuring the potential of the $AgCl-$wire immersed in that *KCl* solution.

Association-Induction Hypothesis (AIH) is a theory of living cell activity but long-forgotten. Unlike membrane theory, AIH attributes the origin of membrane potential to the spatial fixation of mobile ions by their adsorption to the adsorption sites [1]. Firstly, we dare to explain the experimental observation of Fig. 3 using the AIH. The Cl^- in

the KCl solutions could adsorb on the $AgCl-$wires in the Left and the Right phase KCl solutions in $KCl-$sys. According to the AIH, the Cl^- adsorbed on the $AgCl-$wire must be responsible for the $AgCl-$wire potential generation, and K^+ has basically nothing to do with the potential generation. However, the electroneutrality should hold. Therefore, the horizontal axis of Fig. 3 can be interpreted as $-\log_{10}[Cl^-]$ (and $-\log_{10}[K^+]$) as well as $-\log_{10}[KCl]$. The data in Fig. 3 is approximated by the second-order equation as Eq. 2. It is the calibration curve which can relate the $AgCl-$wire potential to $[Cl^-]$ (= $[K^+]$ = $[KCl]$) mathematically.

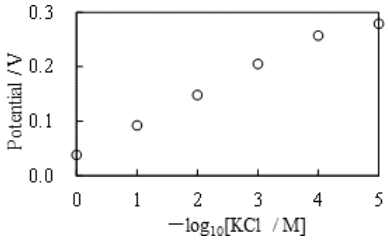

Figure 3. Experimentally obtained relationship, $AgCl-$wire surface potential vs. $-\log_{10}[Cl^-]$

$$V = -0.003(-\log_{10}[Cl^-])^2 + 0.066(-\log_{10}[Cl^-]) + 0.034 \quad (2)$$

Figure 3 suggests that the lower KCl concentration elevates the $AgCl-$wire potential. If there exist no ions in an aqueous solution, the potential of $AgCl-$wire is positive and maximal, but the increase of ion concentration lowers the potential of $AgCl-$wire. The maximal potential state corresponds to the state of "zero $[KCl]$" in Fig. 4. We can interpret this state as the $AgCl-$wire surface bears a certain quantity of "hypothetical" positive charge in pure water and the maximal voltage "V_0" (see Fig. 4) is generated [4]. Then, once the KCl concentration elevates, a small quantity of Cl^- comes to adsorb on the $AgCl-$wire surface as shown in the state of "low $[KCl]$" in Fig. 4. The negative charges of Cl^-'s neutralize the hypothetical positive charges. Therefore, a bit lower voltage "V_ℓ" (see Fig. 4) generates. Further increase of KCl concentration promotes the Cl^- adsorption, resulting in further neutralizing the hypothetical positive charge of $AgCl-$wire. Consequently, even lower potential "V_h" generates as illustrated as the state of "high $[KCl]$" in Fig. 4.

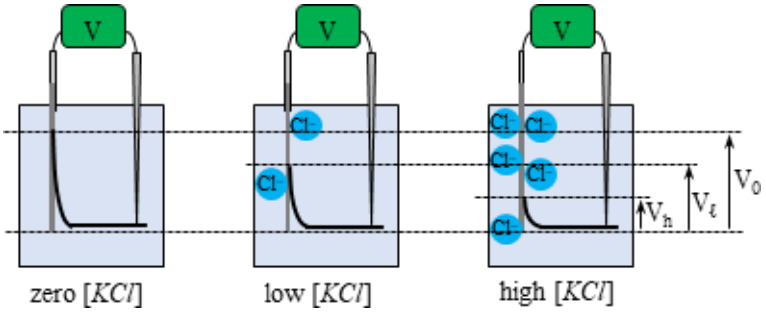

Figure 4. Expected potential profiles (represented by solid curved) around the $AgCl-$wire when the experiment shown in Fig. 1 is performed Bulk phase potential sufficiently far away from the $AgCl-$wire is defined as zero potential.

4.2. Potential across the impermeable membrane

Dashed line in Figure 5 (A), (B) and (C) show the potentials across a Nohole-memb, a 0.3hole-memb and a 2hole-memb in $KCl-$sys, respectively. Solid and dotted curves in Fig. 5 (A), (B) and (C) represent the $AgCl-$wire potentials in the Left phase and Right phase, respectively. These potentials are converted into $[Cl^-]$ using Eq. 2. Although Eq.

2 provides with $[Cl^-]$, the calculated $[Cl^-]$ can be interpreted as $[KCl]$, too. The same experiments for obtaining Fig. 5 were performed using $NaCl-$sys, and the experimental outcomes are shown in Fig. 6. Fig. 6 (A), (B) and (C) can provide with the time course of $[Cl^-]$ as shown in Fig. 6 (a), (b) and (c), respectively, and it can be further interpreted as the time course of $[NaCl]$. Another same experiments were performed using $CaCl_2-$sys. The experimental outcomes are shown in Fig. 7. Fig. 7 (A), (B) and (C) can be interpreted as the time course of $[Cl^-]$ as shown in Fig. 7 (a), (b) and (c), respectively, and it can be further interpreted as the time course of the $CaCl_2$ concentration. But we have to bear in mind that the calculated $[Cl^-]$ can be interpreted as $1/2[CaCl_2]$ rather than $[CaCl_2]$, since $CaCl_2$ dissociates into Ca^{2+} and Cl^- as expressed by Eq. 3.

$$CaCl_2 \longleftrightarrow Ca^{+2} + 2Cl^- \tag{3}$$

Prior to discussing the experimental data in Fig. 5 $\sim$ Fig. 7, we have to make the following comments by taking up Fig. 5 as an example: Fig. 5 (b) shows that $-\log_{10}[Cl^-]$ at $t = 0s$ is greater than $10^{-4}M$, and it is against the experimental initial condition. But it is not false data because of the following reason: Before starting the actual measurement, KCl solutions were supplied into both Left and Right phases. Immediately after that, these solutions inevitably diffused to the other phase through the hole of membrane. Therefore, the KCl concentration at $t = 0s$ comes to differ from the concentration of KCl solutions prepared. It is true for Fig. 5 (c), too, and this explanation is true for both Fig. 6 (b), (c) and Fig. 7 (b), (c), too.

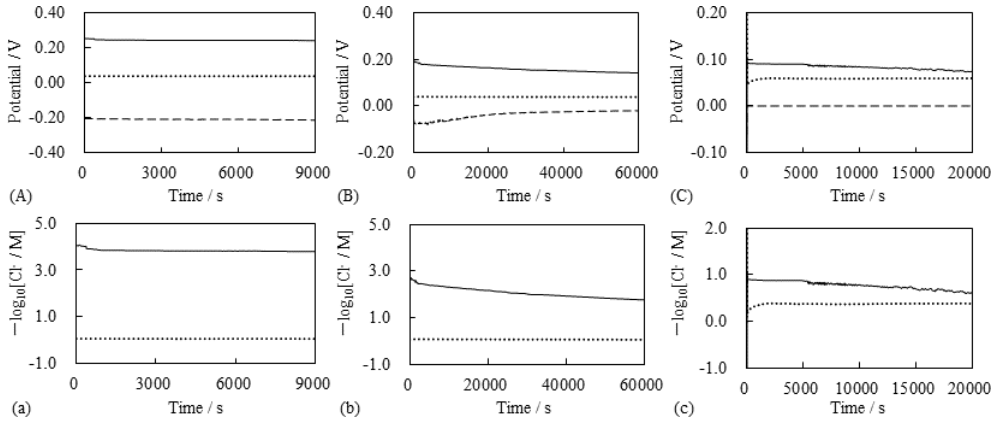

Figure 5. Potential vs. Time and $[Cl^-]$ vs. Time in the $KCl-$sys. (A) and (a): Nohole-memb in use (B) and (b): 0.3hole-memb in use (C) and (c): 2hole-memb in use [In (A), (B) and (C)] Dashed curve: membrane potential across the membrane Solid curve: $AgCl-$wire surface potential in Left phase Dotted curve: $AgCl-$wire surface potential in Right phase [In (a), (b) and (c)] Solid curve: $[Cl^-]$ in the left phase Dotted curve: $[Cl^-]$ in the right phase

Potential across the Nohole-memb First of all, we analyze the data in Fig. 5 (a). Since KCl solutions in the Left and Right phases never diffuse into the other phase due to the membrane impermeability, it is intuitively acceptable that the potential across Nohole-memb is constant as shown in Fig. 5 (A). Figure 5 (A) can provide the time course of ion concentration in both Left and Right phases as in Fig. 5 (a). It is quite interesting that the GHK eq. can reproduce the potential between these two phases by using the ion concentration data in Fig. 5 (a) and assuming $P_{Cl} >> P_K$. The GHK eq. is given by Eq. 4 in this case.

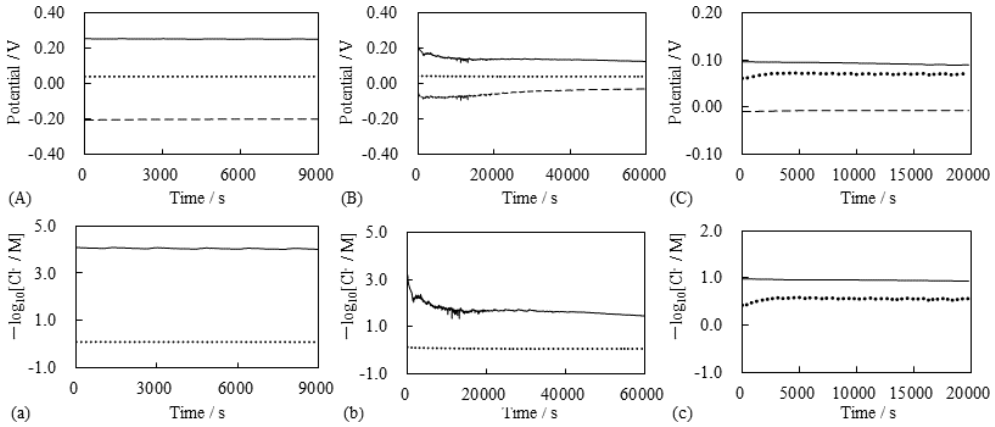

Figure 6. Potential vs. Time and $[Cl^-]$ vs. Time in the $NaCl-$sys. (A) and (a): Nohole-memb in use (B) and (b): 0.3hole-memb in use (C) and (c): 2hole-memb in use [In (A), (B) and (C)] Dashed curve: membrane potential across the membrane Solid curve: $AgCl-$wire surface potential in Left phase Dotted curve: $AgCl-$wire surface potential in Right phase [In (a), (b) and (c)] Solid curve: $[Cl^-]$ in the left phase Dotted curve: $[Cl^-]$ in the right phase

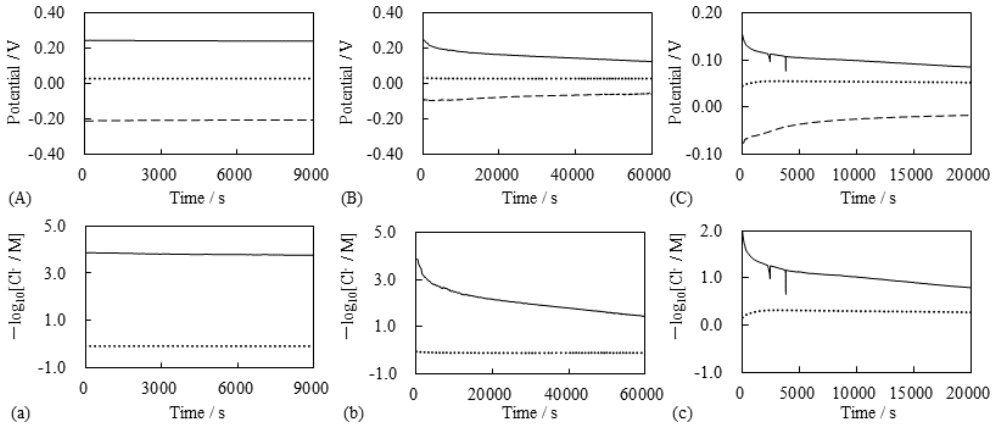

Figure 7. Potential vs. Time and $[Cl^-]$ vs. Time in the $CaCl_2-$sys. (A) and (a): Nohole-memb in use (B) and (b): 0.3hole-memb in use (C) and (c): 2hole-memb in use [In (A), (B) and (C)] Dashed curve: membrane potential across the membrane Solid curve: $AgCl-$wire surface potential in Left phase Dotted curve: $AgCl-$wire surface potential in Right phase [In (a), (b) and (c)] Solid curve: $[Cl^-]$ in the left phase Dotted curve: $[Cl^-]$ in the right phase

$$V_{KCl} = -\frac{kT}{e} ln \frac{P_K[K^+]_i + P_{Cl}[Cl^-]_o}{P_K[K^+]_o + P_{Cl}[Cl^-]_i} \sim -\frac{kT}{e} ln \frac{P_{Cl}[Cl^-]_o}{P_{Cl}[Cl^-]_i} = -\frac{kT}{e} ln \frac{[Cl^-]_o}{[Cl^-]_i} \quad (4)$$

Of course, taking into account a non-zero permeability of the membrane to ions does not make sense, since the Nohole-memb is impermeable. However, the GHK eq. can reproduce the $-0.223V$ potential. Thus, Eq. 4 can reproduce the experimental potential by adjusting the permeability coefficient, even though it is a physically meaningless permeability coefficient. It could be argued that the use of the GHK eq. when using an impermeable membrane is inappropriate from the start. However, even if the permeable membrane is used, the actual measured permeability coefficient is not necessarily used to calculate the GHK eq. [4,17–19]. Often, the permeability coefficient is simply estimated so that the GHK eq. can reproduce the experimentally measured potential, as discussed in the section 1. Therefore, one cannot help but doubt the foundation of the GHK eq., or rather of membrane theory.

As described earlier, the AIH is an alternative but long-forgotten theory to the membrane theory, but its scientific soundness has accumulated in recent times [10,13,20–22]. Here, we explain the behaviour of the membrane potential in Fig. 5 (a) using the AIH. The membrane surfaces of Nohole-members are coated with $AgCl$. Therefore, adsorption of Cl^- on the membrane surface can take place and the expected potential profile is in the illustration in Fig. 8. Consequently, the nonzero potential at the membrane left surface in reference to the bulk phase, V_L, generates and the nonzero potential at the membrane right surface, V_R, generates, too, in Fig. 8. Therefore, AIH predicts that the potential across the membrane, V_{KCl}, by Eq. 5.

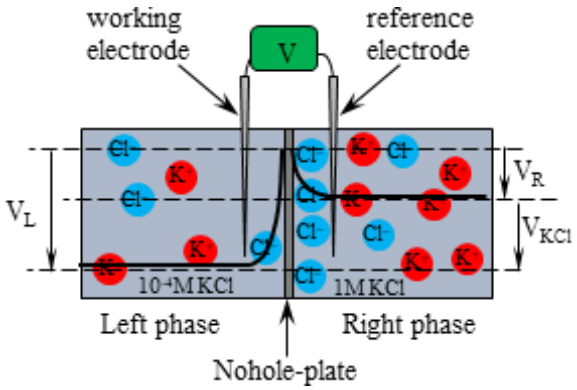

Figure 8. Ion adsorption and expected potential profiles (Solid curves) Membrane surface potential is defined zero.

$$V_{KCl} = V_L - V_R \quad (5)$$

AIH states that V_L depends only on the Left phase condition and V_R depends only on the Right phase condition. Namely, V_L and V_R are independently determined each other. So the V_L is under the influence only of spatially fixed Cl^- adsorbed on the left surface of the membrane, and the V_R is under the influence only of spatially fixed Cl^- adsorbed on the right surface of the membrane, too. We measured the membrane potential V_{KCl} directly, and the outcome is shown in Fig. 5 (A). But can we know V_L and V_R individually? Yes, it is possible. We made measurement of $AgCl-$wire potential shown in Fig. 5 (A) for obtaining the time course of KCl concentration shown in Fig. 5 (a). Fig. 9 illustrates the potential profiles of the membrane and those at the immediate neighbor of $AgCl-$wires. Since the membrane surface and the $AgCl-$wire surface are made of same substance silver oxide, the potential V_L^{ele} of $AgCl-$wire surface in the Left phase must be same as $-V_L$ as

illustrated in Fig. 9, and V_R^{ele} must be also same as $-V_R$ owing to the same reason. These relationships are of course given by Eqs. 6 and 7. Hence, Eq. 5 can be further arranged into Eq. 8. Plugging the experimental data of V_L^{ele} and V_R^{ele} shown in Fig. 5 (A) into Eq. 8, the membrane potential, V_{KCl}, is computed. This computed potential and the experimental membrane potential which is shown in Fig. 5 (A) are shown in the same diagram Fig. 10 (a), and they are in perfect agreement with each other.

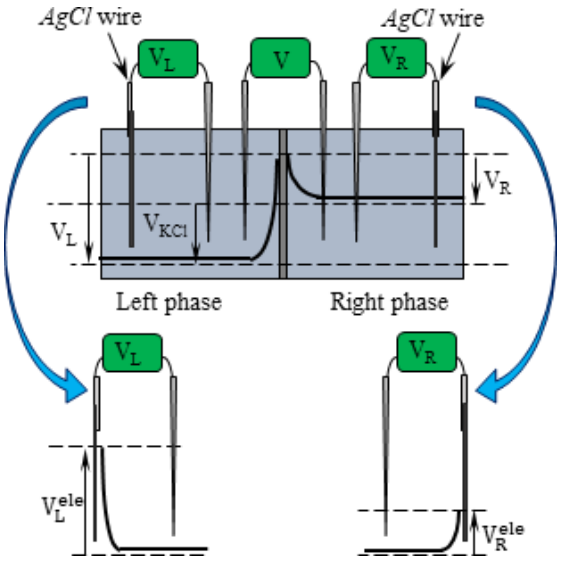

Figure 9. Profiles of membrane potential and the potential at the immediate neighbor of $AgCl-$wires in the experimental setup shown in Fig. 2

$$V_L = -V_L^{ele} \tag{6}$$

$$V_R = -V_R^{ele} \tag{7}$$

$$V_{KCl} = V_L - V_R = (-V_L^{ele}) - (-V_R^{ele}) = V_R^{ele} - V_L^{ele} \tag{8}$$

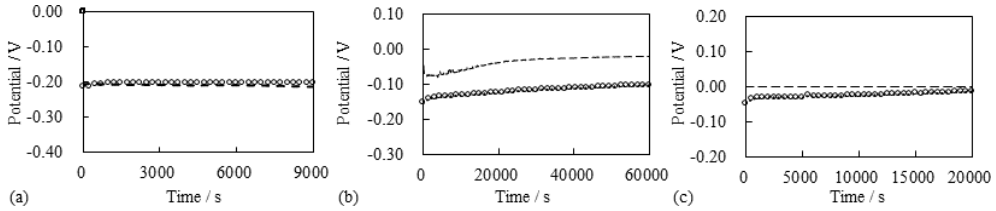

Figure 10. Membrane potential vs. Time where the solutions contain KCl. Dashed curve: Experimental Circle: Calculated (a) Nohole-memb in use (b) 0.3hole-memb in use (c) 2hole-memb in use

The discussion so far described is fully applicable to the potential characteristics of $NaCl-$sys shown in Fig. 6 (A) and (a). Namely, the Cl^- adsorbed on the Nohole-plate is responsible for the potential generation. The potential across the Nohole-plate also can be reproduced computationally using Eq. 8 as shown in Fig. 11 (a) perfectly. Exactly the same discussion is applicable to the $CaCl_2-$sys, too, as shown in Fig. 12 (a). We have to make a

comment on these two diagrams, Figs. 11 (a) and 12 (a), more. The experimentally used solution for obtaining these diagrams was not KCl but $NaCl$ and $CaCl_2$. However, the characteristics of the experimental outcomes are basically all explicable by the adsorption of Cl^-, and the cations are not involved at all. Nevertheless, everything appears to be in harmony with each other. Such characteristics are all fully in harmony with the AIH.

4.3. Potential across the permeable membrane

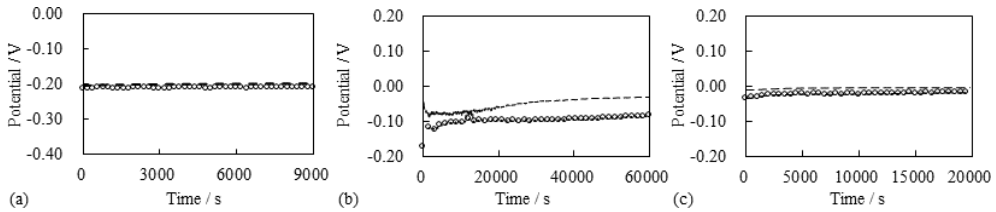

Figure 11. Membrane potential vs. Time where the solutions contain $NaCl$. Dashed curve: Experimental Circle: Calculated (a) Nohole-memb in use (b) 0.3hole-memb in use (c) 2hole-memb in use

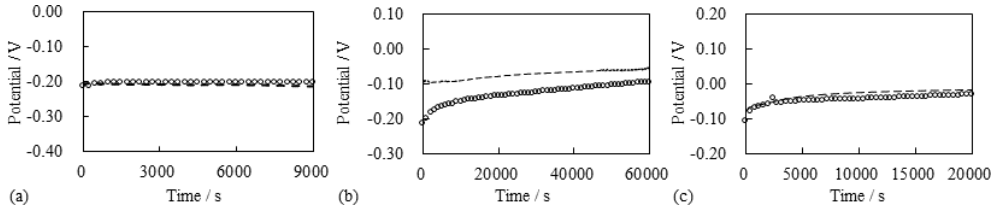

Figure 12. Membrane potential vs. Time where the solutions contain $CaCl_2$. Dashed curve: Experimental Circle: Calculated (a) Nohole-memb in use (b) 0.3hole-memb in use (c) 2hole-memb in use

Potential across the 0.3hole-memb The same experiment described so far was performed using the 0.3hole-memb in place of the Nohole-memb as a membrane of $KCl-$sys. The result is shown in Fig. 5 (B) and (b). Since the K^+ and Cl^- in the Left phase into the Right phase through the tiny hole of 0.3hole-memb by following the law of diffusion, the Left phase KCl concentration was expected to increase, and it was confirmed as shown in Fig. 5 (b). Since the Right phase KCl concentration is extremely high, the visible change of KCl concentration in the Right phase was not observed. We found that it was unable to computationally reproduce the membrane potential V_{KCl} in Fig. 6 (B) using Eq. 8. But the AIH can explain again such a disagreement between the experimental and theoretical membrane potential in the $KCl-$sys as follows: K^+ and Cl^- diffuse little by little through the tiny hole of 0.3hole-memb from the Right phase to the Left phase as illustrated in Fig. 13 till the concentration of both phase reaches the same each other. During the potential measurement, we did not agitate the KCl solution in both phases. Since the diffusion is not the fast process, the KCl concentration gradient inevitably takes place in the Left phase, that is, the most of K^+ and Cl^- coming from the Right phase into the Left phase stay in the vicinity of left surface of 0.3hole-memb as indicated by the solid arrows in Fig. 13. These ions don't so immediately diffuse far away against the indication by the dashed arrow in Fig. 13. Therefore, $[Cl^-]$ at the bulk area of Left phase where the $AgCl-$wire potential was measured was by far lower than $[Cl^-]$ at the left surface of the 0.3hole-memb. However, the $[Cl^-]$ is calculated using the potential data measured by the $AgCl-$wire. Hence, $[Cl^-]$ at the immediate neighbor of 0.3hole-memb left surface must be totally different from the calculated $[Cl^-]$. Therefore, V_L must be totally different from $-V_L^{ele}$. Nevertheless, the potential represented by "$\circ$" in Fig. 10(b) was obtained assuming $V_L = -V_L^{ele}$. Therefore, there is a significant disagreement between the Experimental and Calculate potentials as

in Fig. 10(b). The same explanation is true for the potentials of $NaCl-$sys and $CaCl_2-$sys respectively shown in Figs. 11(b) and 12(b).

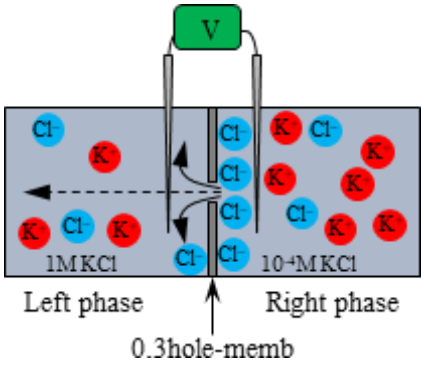

Figure 13. Ion diffuse through the tiny hole from the Right phase to the Left phase

Potential across the 2hole-memb Potentials, when the 2hole-memb in use as a membrane for the $KCl-$sys, are shown in Fig. 10(c). Although the 2hole-memb has a hole at its center like the the 0.3hole-memb, the calculated potential is in good agreement with the experimental potential as shown in Fig. 10(c). Such a good agreement is similar to the potential when the Nohole-memb in use as shown in Fig. 10(a) unlike the potential when the 0.3hole-memb in use. It is explicable by the AIH again. Since the diameter of 2hole-memb is so large that the large quantity of K^+ and Cl^- in the Right phase can diffuse to the Left phase immediately. Namely, the flux of K^+ and Cl^- is by far greater when the 2hole-memb is used compared with the flux when the 0.3hole-memb is used. Hence, $[KCl]$ is approximately same everywhere in both phases. Hence, the degree of Cl^- adsorption on the left surface of 2hole-memb is basically same as the degree of Cl^- on the $AgCl-$wire in the Left phase. Therefore, Eq. 6 is basically right, and of course Eq. 7 is valid. Hence, the calculated potential is in good agreement with the experimental potential when the $KCl-$sys is employed, as shown in Fig. 10(c). The same discussion is applicable for the potential profiles shown in Figs. 11(c) and 12(c).

4.4. Potentials in the AIH purview

What we have shown here says that even the use of impermeable membrane causes the highest magnitude of membrane potential. In contrast, the membrane theory suggests the membrane permeability is fundamentally necessary for nonzero membrane potential generation. So, there is a disagreement between the membrane theory and the experimental observation. There is one other disagreement: The membrane theory states that the ion selectivity of the membrane permeability is necessary for the nonzero membrane potential generation. Both 0.3hole-memb and 2hole-memb are permeable to ions but they cannot exhibit the ion selectivity at all. Nevertheless, the nonzero membrane potentials were generated across them as shown in Figs. 5(b) (c), 6(b) (c) and 7(b) (c).

To sum up, the membrane theory states that the membrane permeable to mobile ions with the ion selectivity can exhibit the clear nonzero membrane potential, but the experimental observation suggests that the greater magnitude of membrane potential is achieved by using a less permeable and non-ion-selective membrane. This disagreement can be amended only by the AIH as we describe for every experimental potential behavior earlier. So, the potential generation by the spatial fixation of charges of ions by ion adsorption is the primary cause of membrane potential.

5. Conclusions

It is broadly acknowledged that the cause of membrane potential generation lies in the membrane selective permeability to mobile ions. It is the membrane potential generation

mechanism taking root in the membrane theory. However, the experimental facts shown in this paper are fully conflict with the prediction by the membrane theory. On the other hand, the membrane potential generation mechanism based on the AIH is in full harmony with the experimental fact. Why do we need to neglect the AIH? Experimental fact says that that the AIH can serve as a membrane potential generation mechanism. We believe it worthwhile reinvestigating the membrane potential generation mechanism, and at least, the membrane theory is incomplete.

Author Contributions: Conceptualization, H.T.; Methodology, H.T; Validation, H.T. and B.D.; Investigation, H.T. and B.D.; Data curation, H.T.; Writing—original draft preparation, H.T.; Writing—review and editing, H.T. and B.D.; All authors have read and agreed to the published version of the manuscript.

Funding: This research received no external funding.

Conflicts of Interest: The authors declare no conflict of interest.

References

1. Gilbert N. Ling. *A Revolution in the Physiology of the Living Cell*; Krieger Pub Co, Malabar, Florida, 1992.
2. James Keener, James Sneyd. *Mathematical Physiology: I: Cellular Physiology (Interdisciplinary Applied Mathematics)*; Springer, 2008.
3. G. Bard Ermentrout, David H. Terman. *Mathematical Foundations of Neuroscience (Interdisciplinary Applied Mathematics Book 35*; Springer, 2010.
4. H. Tamagawa, K. Ikeda. Another interpretation of Goldman-Hodgkin-Katz equation based on the Ling's adsorption theory. *Eur. Biophys, J.* **2018**, *47*, 869–879.
5. H. Tamagawa. Mathematical expression of membrane potential based on Ling's adsorption theory is approximately the same as the Goldman–Hodgkin–Katz equation. *J. Biol. Phys.* **2018**, *45*, 13–30.
6. H. Tamagawa, T. Mulembo, B. Delalande. What can S-shaped potential profiles tell us about the mechanism of membrane potential generation? *Euro. Biophys, J.* **2021**. doi:10.1007/s00249-021-01531-7.
7. H. Tamagawa, T. Mulembo, B. Delalande. The need of the reconsideration of generation mechanism of membrane potential by mean of the Ling's adsorption theory. *Eur. Biophys. J.* **2021**. doi:10.1007/s00249-021-01526-4.
8. Seong G. Hwang, Jun Ki Hong, Abha Sharma, Gerald H. Pollack, Gun Woong Bahng. Exclusion zone and heterogeneous water structure at ambient temperature. *PLoS ONE* **2018**, *13, Paper No. e0195057*. doi:doi.org/10.1371/journal.pone.0195057.
9. Kelath Murali Manoj, Vidhu Soman, Vivian David Jacob, Abhinav Parashar, Daniel Andrew Gideon, Manish Kumar, Afsal Manekkathodi, Surjith Ramasamy, Kannan Pakshirajan, Nikolai Mikhailovich Bazhin. Chemiosmotic and murburn explanations for aerobic respiration: Predictive capabilities, structure-function correlations and chemico-physical logic. *Archives of Biochemistry and Biophysics* **2019**, *676, Paper No. 108128*.
10. Magdalena Kowacz, G.H.P. Cells in New Light: Ion Concentration, Voltage, and Pressure Gradients across a Hydrogel Membrane. *AOS OMEGA* **2020**, *5*, 21024–21031.
11. Kelath Murali Manoj, Vivian David Jacob. THE MURBURN PRECEPTS FOR PHOTORECEPTION. *Biomedical Reviews* **2020**, *31*, 67–74. doi.org/10.1016/j.jpap.2020.100015.
12. Luis A. Bagatolli, Roberto P. Stock. Lipids, membranes, colloids and cells: A long view. *BBA - Biomembranes* **2021**, *1863, Paper No. 183684*. doi:doi.org/10.1016/j.bbamem.2021.183684.
13. Luis A. Bagatolli, Agustín Mangiarotti, Roberto P. Stock. Cellular metabolism and colloids: Realistically linking physiology and biological physical chemistry. *Progress in Biophysics and Molecular Biology* **2021**, *162*, 79–88. doi:doi.org/10.1016/j.pbiomolbio.2020.06.002.
14. Kelath Murali Manoj, Afsal Manekkathodi. Light's interaction with pigments in chloroplasts: The murburn perspective. *Journal of Photochemistry and Photobiology* **2021**, *5, Paper No. 100015*.
15. Khalid R. Temsamani, K. Lu Cheng. Studies of chloride adsorption on the Ag/AgCl electrode. *Sensors and Actuators B* **2001**, *76*, 551–555.
16. Hirohisa Tamagawa, Sachi Morita. Membrane Potential Generated by Ion Adsorption. *Membranes* **2014**, *4*, 257–274. doi:10.3390/membranes4020257.
17. E. M. Eright, J. M. Diamond. Efects of pH and polyvalent cations on the selective permeability of gall-bladder epithelium to mono valent ions. *Biochim. Biophys. Acta* **1968**, *163*, 57–74.

18. Andrea Olschewski, Horst Olschewski, Michael E. Bräu, Gunter Hempelmann, Werner Vogel, Boris V. Safronov. Basic Electrical Properties of In situ Endothelial Cells of Small Pulmonary Arteries during Postnatal Development. *Am. J. Respir. Cell Mol. Biol.* **2001**, *25*, 285–290.
19. Victor V. Uteshev. Evaluation of Ca^{2+} permeability of nicotinic acetylcholine receptors in hypothalamic histaminergic neurons. *Acta Biochim. Biophys. Sin.* **2010**, *42*, 8–20. doi:10.1093/abbs/gmp101.
20. Gary E. Wnek. Perspective: Do Macromolecules Play a Role in the Mechanisms of Nerve Stimulation and Nervous Transmission? *JOURNAL OF POLYMER SCIENCE, PART B: POLYMER PHYSICS* **2015**, *54*, 7–14.
21. Laurent Jaeken. The neglected functions of intrinsically disordered proteins and the origin of life. *Progress in Biophysics and Molecular Biology* **2017**, *126*, 31–46. doi.org/10.1016/j.pbiomolbio.2017.03.002.
22. Vladimir V. Matveev. Cell theory, intrinsically disordered proteins, and the physics of the origin of life. *Progress in Biophysics and Molecular Biology* **2019**, *149*, 114–130. doi.org/10.1016/j.pbiomolbio.2019.04.001.